PSpice Simulation of Surge Testing for Electrical Vehicles

Xiaofeng Pan, Thomas Rinkleff
Dept. EEIZ, EMV-Zentrum,
Forschung & Entwicklung,
Brieffach 17320, Volkswagen AG
D38436 Wolfsburg, Germany

Benjamin Willmann, Ralf Vick
Institut für Grundlagen der Elektrotechnik
und Elektromagnetische Verträglichkeit (IGET),
Otto-von-Guericke-Universität Magdeburg
D39016 Magdeburg, Germany

***Abstract*—In this paper a general modeling procedure for 1.2/50µs generator defined in IEC 61000-4-5 is presented. Subsequently, in PSpice this surge generator model is employed in order to simulate and observe surge tests for electrical vehicles, which have plugs to the public mains supply due to their charging systems. In the research several shielding set-ups of charging systems in electrical vehicles are defined and studied from the EMC aspect. Comparing to measurement results the PSpice simulation always offers a good prediction and agreement to different research set-ups.**

Keywords-Pspice modeling; Surge; Electrical Vehicles; Charging system

I. INTRODUCTION

Nowadays, because of the advantage of zero CO_2 emission, electrical vehicles (EV) have been a new innovation in the automobile industry. Therefore, the high power electrical driving system in EV brings EMC engineers plenty of new challenges, which could not be easily clarified and solved like traditional EMC problems in 12V vehicle power systems.

For example, the high power battery in EV is normally charged with 230V public mains supply. By means of this charging an electrical connection between the vehicle and the public supply network is built up. Now under the consideration of electromagnetic immunity it seems to be a great risk, when a surge appears in the 230V network and is coupled through charging cables into 12V vehicle power systems, because the automobile electronics, especially their ICs, could be easily damaged by such an overvoltage. Until now there are still few observations or researches on this problem in the automobile industry, because the traditional vehicles never had a connection to 230V network and thus the standard surge requirements to 230V supply network, e.g. IEC 61000-4-5, is not taken account at all in current automobile EMC tests.

In this paper it is attempted to join the surge test defined in IEC 61000-4-5 with electrical vehicles by means of numerical simulation. Principally a surge can always be described as a double exponential function impulse. From previous researches in [1], [2] and [3] different mathematical algorithms are implemented and discussed in order to characterizing the double exponential waveform. However, the characteristic parameters in these researches have no physical meanings. It is very difficult to establish a physical circuit directly from these parameters to generate arbitrary double exponential waves for different surge tests. For this purpose, first of all, a general method to characterize the surge waveform according to requirements in IEC 61000-4-5 is introduced. With the help of this method a 1.2/50µs surge generator is modeled and parameterized in PSpice. Then the established PSpice model of the generator is applied to simulate surge tests on high voltage cables in order to observe the coupling from them into normal 12V cables in vehicles. For researches with different set-ups the simulation shows always a good agreement to measurements. It also helps EMC development engineers in the automobile industry to obtain the primary experience, how the potential surge problem caused by charging of electrical vehicles should be taken into account and how its risk could be reduced.

II. MODELING OF SURGE GENERATOR

There are two different surge waveforms defined in IEC 61000-4-5, namely 1.2/50µs surge for power lines and 10/700µs surge for communication cables. Because the high voltage cables in electrical vehicles only serve as high power traction lines, the 1.2/50µs surge is chosen here as the observed overvoltage, which according to IEC 61000-4-5 can be generated with the following equivalent circuit in Fig. 1.

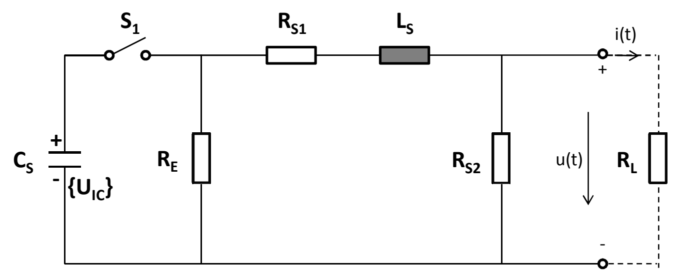

Fig. 1: Equivalent circuit of 12/50µs surge generator

The elements in Fig. 1 could be physically explained as below [4]:

- C_S: storage conductance with an initial voltage U_{IC};
- S_1: switch of discharging circuit;
- L_S: rising time forming inductance;
- R_E, R_{S2}: impulse forming resistance;

978-1-4673-0717-8/12/$31.00 ©2012 IEEE

- R_{S1}: matching resistance;
- R_L: load resistance;

In the standard, instead of specification of the element parameters, only some general requirements to waveforms at the circuit output are given:

1. The open load voltage ($R_L = \infty$) must have 1.2µs±30% wave-front steepness (T_1) and 50µs±20% time to half value of the wave tail (T_2);
2. The short circuit current ($R_L = 0$) must have 8µs±20% by T_1 and 20µs±20% by T_2.
3. The peak value of open voltage U_{max}^{open} is defined on different levels, e.g. 500V, 1kV and 2kV. The requirement to corresponded short circuit current I_{max}^{short} is always the halves of the voltage value, e.g. 250A, 500A and 1kA.

It is easy to know that the circuit in Fig.1 generates actually double exponential impulses at its output. Theoretically the relations between the circuit elements and the output waveform in Fig. 1 could be written as [5]:

$$\begin{cases} \dfrac{L_S}{R_{S1}+R_{S2}} = \tau_{rise}^{open} & (Eq.1) \\ \dfrac{R_E \cdot (R_{S1}+R_{S2})}{R_E + (R_{S1}+R_{S2})} \cdot C_S = \tau_{fall}^{open} & (Eq.2) \\ \dfrac{L_S}{R_{S1}} = \tau_{rise}^{short} & (Eq.3) \\ \dfrac{R_E \cdot R_{S1}}{R_E + R_{S1}} \cdot C_S = \tau_{fall}^{short} & (Eq.4) \end{cases}$$

Based on Eq. 1 – Eq. 4 the dependence between the circuit elements in Figure 1 can be described as:

$$\begin{cases} R_{S1} = k_1 \cdot L_s = \dfrac{1}{\tau_{rise}^{short}} \cdot L_S & (Eq.5) \\ R_{S2} = k_2 \cdot L_s = \left(\dfrac{1}{\tau_{rise}^{open}} - \dfrac{1}{\tau_{rise}^{short}}\right) \cdot L_S & (Eq.6) \\ R_E = k_3 \cdot L_S \\ = \left(\dfrac{\tau_{fall}^{open} \cdot k_1 \cdot k_2}{\left(\tau_{fall}^{short} - \tau_{fall}^{open}\right) \cdot k_1 + \tau_{fall}^{short} \cdot k_2} - k_1\right) \cdot L_S & (Eq.7) \\ C_S = \dfrac{k_4}{L_S} = \dfrac{\tau_{fall}^{short} \cdot (k_3 + k_1)}{k_3 \cdot k_1} \cdot \dfrac{1}{L_s} & (Eq.8) \end{cases}$$

Mathematically the time constants τ_{rise} and τ_{fall} could be approximated derived from T_1 and T_2:

$$\begin{cases} \tau_{rise} = \dfrac{T_1}{1.25 \cdot 2.2} & (Eq.9) \\ \tau_{fall} = \dfrac{1}{0.693} \cdot (T_2 - T_1) & (Eq.10) \end{cases}$$

Hence from Eq. 9 – Eq. 10 it is known that the coefficients k_1 to k_4 in Eq. 5 – Eq. 8 can be determined by the time parameters T_1^{open}, T_2^{open}, T_1^{short} and T_2^{short}. The circuit parameters R_{S1}, R_{S2} and R_E are linear proportional to the parameter L_S and the parameter C_S is inversely proportional to L_S.

Subsequently, it is necessary to determine the parameter U_{IC} in Fig. 1, which can be derived either from $i^{short}(t)$ or from $u^{open}(t)$. In this paper only the derivation by means of $i^{short}(t)$ is discussed. As already mentioned the short circuit current of the surge generator is a double exponential function, which can be obtained by using the Kirchhoff's law as well as the initial conditions $U(C_s)|_{t=0} = U_{IC}$ and $i(t)|_{t=0} = 0$ of the equivalent circuit in Fig. 1:

$$i^{short}(t) = k^{short} \cdot \left(e^{\lambda_1^{short} \cdot t} - e^{\lambda_2^{short} \cdot t}\right) \qquad (Eq.11)$$

The coefficients λ_1^{short} and λ_2^{short} could be written as:

$$\begin{cases} \lambda_1^{short} = \dfrac{-b^{short} + \sqrt[2]{{b^{short}}^2 - 4 \cdot a^{short} \cdot c^{short}}}{2 \cdot a^{short}} & (Eq.12) \\ \lambda_2^{short} = \dfrac{-b^{short} - \sqrt[2]{{b^{short}}^2 - 4 \cdot a^{short} \cdot c^{short}}}{2 \cdot a^{short}} & (Eq.13) \end{cases}$$

The parameters a^{short}, b^{short} and c^{short} are coefficients of the characteristic equation to the equivalent circuit in Fig. 1, which are obtained by:

$$\begin{cases} a^{short} = L_S \cdot C_S & (Eq.14) \\ b^{short} = R_{S1} \cdot C_S + \dfrac{L_S}{R_E} & (Eq.15) \\ c^{short} = 1 + \dfrac{R_{S1}}{R_E} & (Eq.16) \end{cases}$$

The coefficient k^{short} could be derived from the initial conditions and be written as:

$$k^{short} = \frac{U_{IC}}{(\lambda_1^{short} - \lambda_2^{short}) \cdot L_S} \qquad (Eq.17)$$

Considering the peak current of the double exponential wave, which appears at

$$t_{max}^{short} = \frac{\ln(\lambda_1^{short} / \lambda_2^{short})}{\lambda_2^{short} - \lambda_1^{short}} \qquad (Eq.18)$$

U_{IC} can be determined by t_{max}^{short} and I_{max}^{short}:

$$U_{IC} = \frac{(\lambda_1^{short} - \lambda_2^{short}) \cdot I_{max}^{short} \cdot L_S}{e^{\lambda_1^{short} \cdot t_{max}^{short}} - e^{\lambda_2^{short} \cdot t_{max}^{short}}} \qquad (Eq.19)$$

Because all the parameters in Eq. 19, except for I_{max}^{short}, which has been given in the standard IEC 61000-4-5, are functions of the parameter L_S, the initial condition U_{IC} is in fact analytically determined only by the parameter L_S.

The derivation of U_{IC} from $u^{open}(t)$ is actually similar to the calculation above. However the coefficients in Eq. 14 – Eq. 16 should be substituted with

$$\begin{cases} a^{open} = L_S \cdot C_S & (Eq.20) \\ b^{open} = (R_{S1} + R_{S2}) \cdot C_S + \dfrac{L_S}{R_E} & (Eq.21) \\ c^{open} = 1 + \dfrac{(R_{S1} + R_{S2})}{R_E} & (Eq.22) \end{cases}$$

and the parameter I_{max}^{short} in Eq. 19 is replaced by U_{max}^{open}/R_{S2}.

From the mathematical derivation above it is known that the physical parameters of the equivalent circuit in Fig. 1 are able to be completely determined by the parameter L_S, if the requirements on waveforms in IEC 61000-4-5 are given. The parameters R_{S1}, R_{S2} as well as R_E are linear proportional to L_S (Eq. 5 – Eq. 7). The parameters C_S and U_{IC} are non-linear dependent on L_S (Eq. 8 and Eq. 19). In order to determine L_S, numerical optimization approaches, such like Least-Mean-Square Algorithm in this paper, could be used. The error function between calculation and measurement is expressed as

$$\delta^2 = \sum_{n=0}^{N} (i_{cal}^{short}(t_n, L_S) - i_{meas}^{short}(t_n))^2 + \sum_{m=0}^{M} (u_{cal}^{open}(t_m, L_S) - u_{meas}^{open}(t_m))^2 \quad (Eq. 23)$$

The parameter L_S is finally regressed by minimizing the error function (Eq. 24).

$$L_{S,opt} = L_S|_{\min(\delta^2)} \quad (Eq. 24)$$

Thereby the physical model of the surge generator in Fig. 1 is completely parameterized. For example, to generate a 500V/250A surge with the waveform of $T_1^{open} = 1.2\mu s$, $T_2^{open} = 50\mu s$, $T_1^{short} = 8\mu s$ and $T_2^{short} = 20\mu s$, the parameter $L_{S,opt}$ is given as 5.6µH. The other circuit elements in Fig. 1 can be then determined as following:

- $C_S = 10\mu F$;
- $R_E = 15\Omega$;
- $R_{S1} = 2\Omega$;
- $R_{S2} = 11\Omega$;
- $U_{IC} = 624V$.

Fig. 2 shows the surge waves of open load voltage and short circuit current for this case.

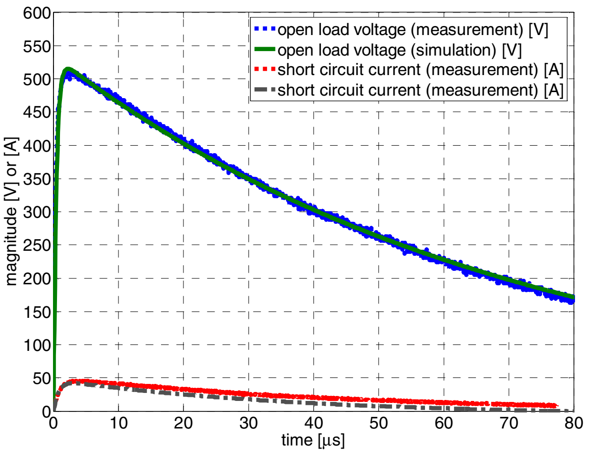

Fig. 2 open load voltage and short circuit current without decoupling network (500V/250A surge)

In surge testing a decoupling network has to be used in order to block the surge back to the 230V main supply (Fig. 3).

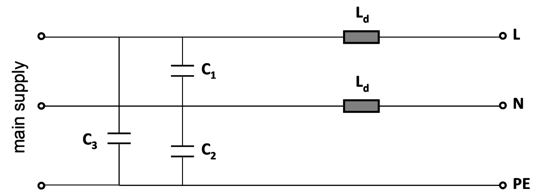

Fig. 3 decoupling network

This decoupling network distorts the actual surge waveform, which is injected into the EUT. Hence its influence during the surge testing must be considered in the simulation. The inductivity L_S in Fig. 3 is already given as 1.5mH in the standard. To determine the coupling capacitance in Fig. 3 the measurements between L - N, N - PE and L -PE are carried out by means of a RLC-meter. The three capacitive parameters C_1, C_2 and C_3, could be easily calculated from these measurements on three different parallel circuits. In this case they are determined as $C_1 = 4.5\mu F$ and $C_2 = C_3 = 9\mu F$. Fig. 4 shows the open load voltage and short circuit current after the decoupling network output (injection between L and PE with a 10Ω/9µF couple network). Comparing to Fig. 2 the open load voltage in Fig. 4 is significantly tightened due the additional decoupling network.

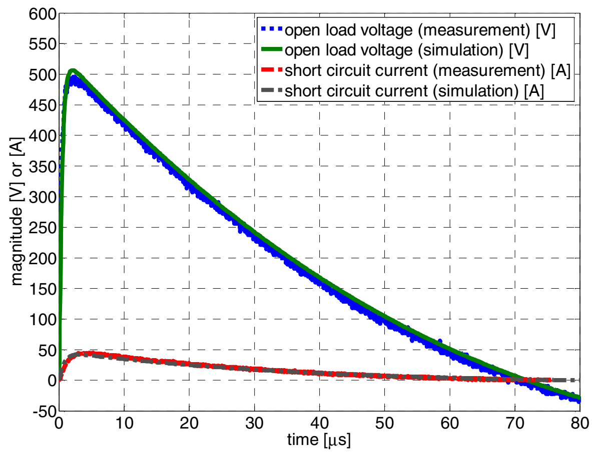

Fig. 4 open voltage and short circuit current with decoupling network (injection between L and PE with a 10Ω/9µF couple network)

III. MODELLING OF EUT

The EUT in this research is constructed of a high voltage cable with braided shields and a simple low voltage wire. To model simple wires over ground plane the classic transmission line theory can be employed. However, the modeling of cables with braided shields becomes more difficult because of the complex couple mechanism between the inner and outer electromagnetic fields of shielded cables. To describe this couple mechanism the transfer impedance and admittance of shielded cables are defined [6]. However, nowadays there are only empirical methods available to calculate these transfer factors. In the presented research the Demoulin method [6] is chosen and applied by modeling the high voltage cable in surge testing. In order to verify the accuracy of the cable modeling, the electromagnetic interference from the shielded high voltage cable to the simple low voltage wire is compared by measurement and simulation (Fig. 5). The equivalent circuit (per unit length) of the cable simulation above is presented then in Fig. 6. In the PSpice simulation here, interactions between inner and outer circuits of the shielded cable are modeled only by means of four transfer factors $z_{t,in}$, $z_{t,out}$, $y_{t,in}$, $y_{t,out}$, which were calculated with the Demoulin formula.

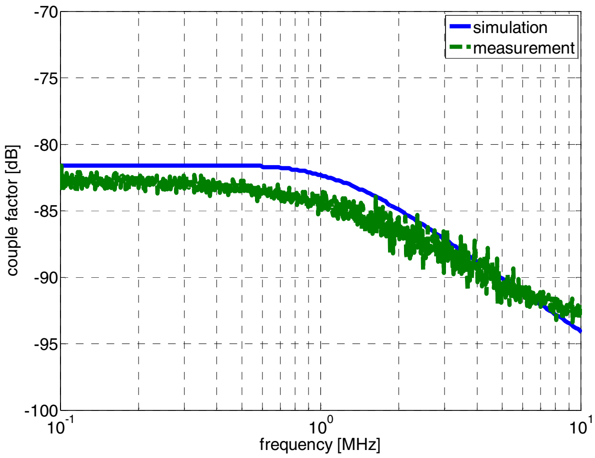

Fig. 5 interference between shielded high voltage cable and unshielded low voltage cable

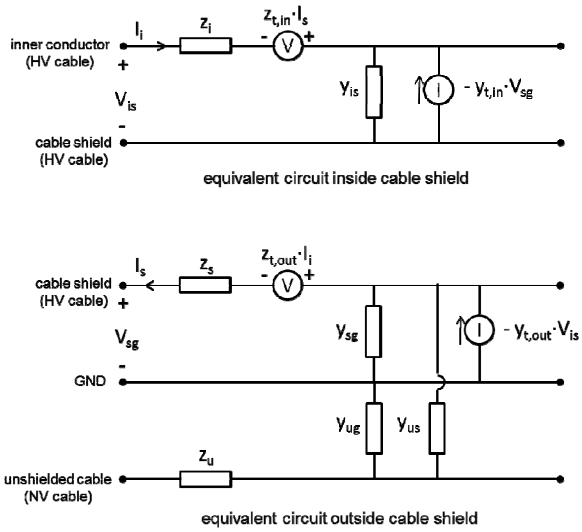

Fig. 6 equivalent circuit (per unit length) of cable simulation in Fig. 5

IV. SET-UP OF SURGE TESTING

Fig. 7 shows the table set-up of surge testing. The tested cables are both 1.5m long and have a distance of 5cm over the ground plane. The unshielded low voltage wire is carried in parallel to the shielded high voltage cable with a distance of 3cm. The surge is injected into one side of the high voltage cable with 500V peak value between the inner conductor of the high voltage cable and the ground plane (PE), respectively as a common-mode disturbance.

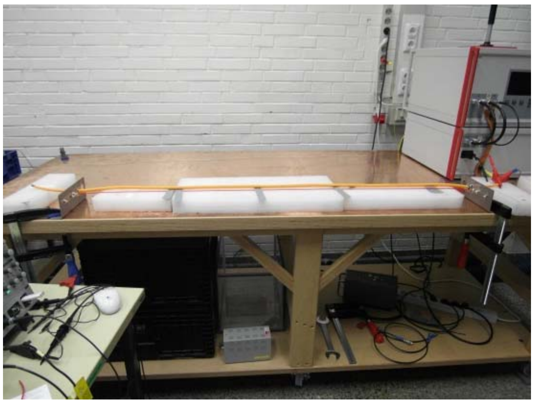

Fig. 7 table set-up of surge testing

In the research, different shield concepts of the high voltage cable are defined, in order to observe how these concepts affect the coupled surge into the parallel low voltage wire. For this purpose the following shield concepts are tested:

- var.1: good ground plane connections of cable shield at both ends;
- var.2: one good ground plane connection of cable shield and the other with a pigtail of 10cm;
- var.3: no ground plane connections of cable shield.

In most literatures the influence of a pigtail is described as a simple inductor. If this assumption is adequate enough to model the pigtail connection in surge testing has still to be examined. In the following the 10cm pigtail in this research is modeled with two approaches:

- Its self-inductance is measured with a LRC-meter and the pigtail itself could be modeled as a simple inductor between cable shield and ground plane (approach 1).
- The pigtail is modeled completely as a wire over ground plane and directly connected to cable shield and ground (approach 2).

Now, the same measurement and simulation for cables in Chapter III, however, this time with 10cm pigtail, were carried out again. Fig. 8 shows the measured and simulated results. It is to see that only the second approach accurately reproduces the influence due to pigtail connections.

In the surge testing, in consideration of the worst-cases of electromagnetic coupling, the high voltage cable and the low voltage wire are loaded with two ways. At the first step, the both are open loaded in order to produce the hardest electric coupling. The coupled voltage on low voltage wire is observed. At the second step, they are short circuited to the ground plane. The observation of the hardest magnetic coupling is then realized by means of the coupled current on low voltage wire. Fig. 9, Fig. 10, Fig. 11 and Fig. 12 are measured and simulated results of these voltages and currents. Comparing the different shield concepts it is to see that without cable shield both the electric and the magnetic coupling are increased significantly. The coupled surge disturbance under this condition could be very harmful to 12V control units in vehicles. Furthermore, a

978-1-4673-0717-8/12/$31.00 ©2012 IEEE

non-ideal shield connection, such like pigtail, is already very helpful to protect 12V control units against the surge damage from high voltage cables in electrical vehicles. However, in the case of high surge currents, the influence of pigtail connections should be taken more account.

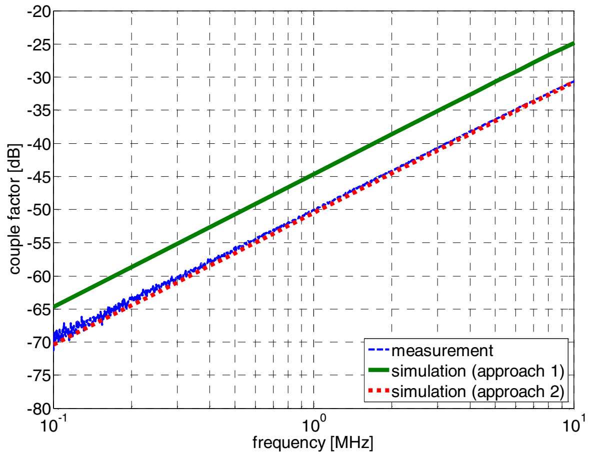

Fig. 8 verification of pigtail modeling

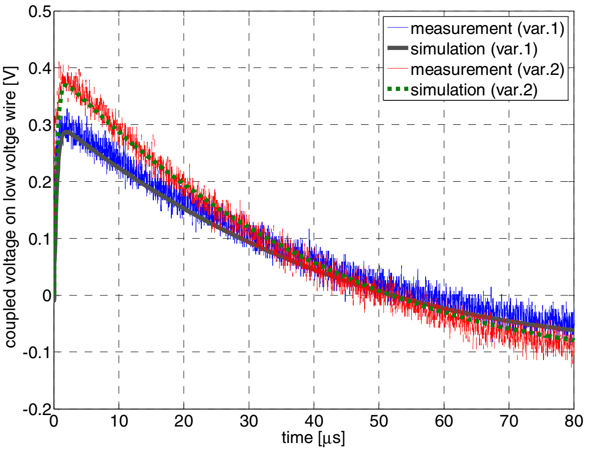

Fig. 9 open load voltage under different shield concepts (var. 1 and var. 2)

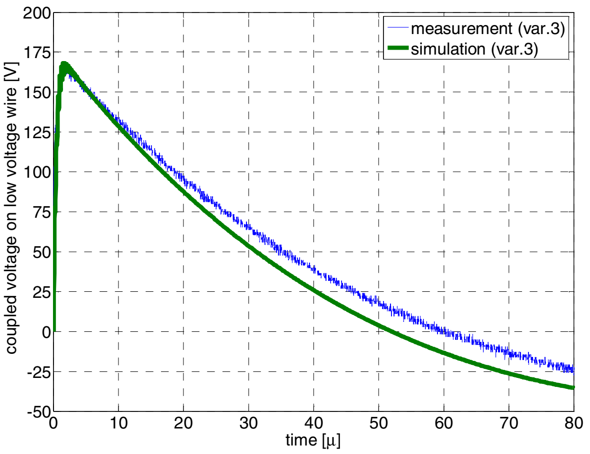

Fig. 10 open load voltage under different shield concepts (var. 3)

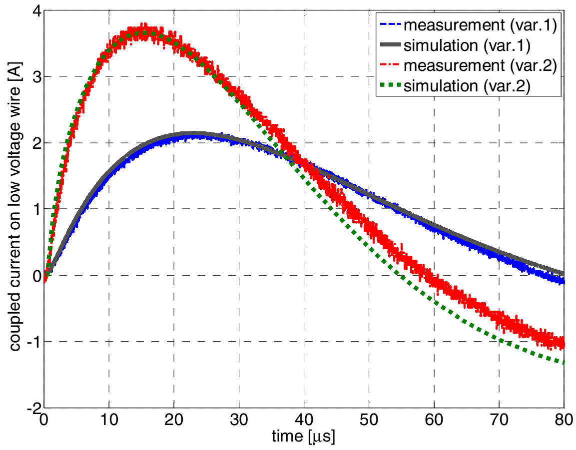

Fig. 11 short circuit current under different shield concepts (var. 1 and var. 2)

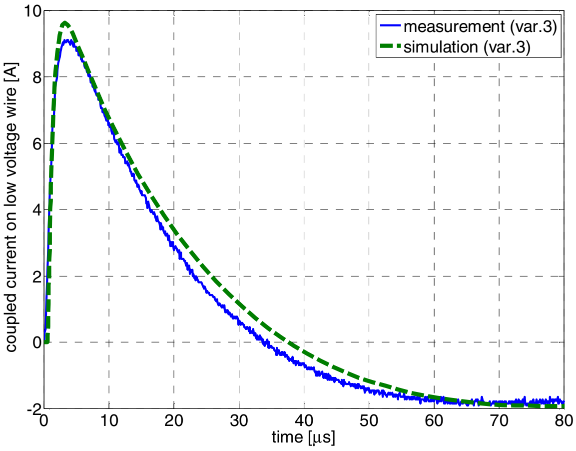

Fig. 12 short circuit current under different shield concepts (var. 3)

V. CONCLUSIONS

In this paper a general semi-analytical modeling procedure for 1.2/50µs surge generator in IEC 61000-4-5 is introduced and verified by means of comparison to measurements.

Based on this model the PSpice simulation for surge testing can be easily carried out in order to observe possible surge problems in electrical vehicles due to the connection of its charging cable with 230V main supply. Through the research on these surge tests, the good validity of the Demoulin method to model shielded high voltage cables in electrical vehicles as well as the accurate approach of pigtail modeling is also proved.

All the simulation results of surge testing have a good agreement with the subsequent measurements on the test table. Both the simulations and the measurements show that the high voltage charging cable should be shielded in order to reduce the surge risk from the main supply via high voltage cable into the 12V vehicle power systems. Only considering the surge problem, a non-optimal pigtail connection of cable shields can also be accepted in practice.

978-1-4673-0717-8/12/$31.00 ©2012 IEEE

Actually, the presented modeling procedure of surge generators in this paper could also be easily extended to researches on other surge generators and even on fast transient impulses, such like burst tests.

REFERENCES

[1] Michael Camp, Heyno Garbe, "*Parameter Estimation of Double Exponential Pulses (EMP, UWB) with Least Squares and Nelder Mead Algorithm*", IEEE Trans. on EMC, vol. 46, no. 4, pp. 675 – 678, Nov. 2004

[2] Congguang Mao, Hui Zhou, "*Novel Parameter Estimation of Double Exponential Pulse (EMP, UWB) by Statiscal Means*", IEEE Trans. on EMC, vol. 50, no. 1, pp. 97 – 100, Feb. 2008

[3] Mathias Magdowski, Ralf Vick, "*Estimation of the Mathematical Parameters of Double–Exponential Pulses Using the Nelder–Mead Algorithm*", IEEE Trans. on EMC, vol. 52, no. 4, pp. 1060 – 1062, Nov. 2010

[4] International Standard IEC 61000–4–5, "*Testing and measurement techniques – Surge immunity test*", 2nd. Edition, Nov. 2005.

[5] Adolf J. Schwab, "*Elektromagnetische Verträglichkeit*," Springer, Berlin, chap. 8.1.3, Mai 1996.

[6] Frederick M. Tesche, Torbjörn Karlsson, Michel V. Ianoz, "*EMC Analysis Methods and Computational Models*", Wiley & Sons, chap. 9, 1996

978-1-4673-0717-8/12/$31.00 ©2012 IEEE